Available online at www.sciencedirect.com

ScienceDirect

Procedia CIRP 78 (2018) 91–96

www.elsevier.com/locate/procedia

6th CIRP Global Web Conference
"Envisaging the future manufacturing, design, technologies and systems in innovation era"

A study on the feasibility of laser annealing to relieve residual stresses in cold spray coatings

Ben Hunter, Barry Aldwell, Richard Jenkins and Rocco Lupoi*

Trinity College Dublin, The University of Dublin, Department of Mechanical & Manufacturing Engineering, Parsons Bulding, Dublin 2, Ireland

* Corresponding author. Tel.: +353-1-8961729; fax: +353-1-6795554; *E-mail address:* lupoir@tcd.ie

Abstract

This paper investigates the effect of laser annealing on residual stresses in cold spray (CS) coatings. Residual stresses can compromise the material properties of the deposited materials, and potentially cause delamination; thus it is essential to understand and reduce these residual stresses where possible. The deposition of single tracks of copper onto aluminium substrates was examined. A novel method of in-situ monitoring of residual stresses during the CS process was developed, using a bondable rectangular strain gauge rosette. A standardised substrate fixing method was designed to ensure consistent and repeatable CS tests, where the in-situ strains were recorded during both the CS and laser annealing process. The experimental results proved that laser annealing is a potential in-process treatment method for relieving residual stresses within a CS coating, when compared to a standard furnace stress relieving cycle. However, results indicated that stresses are reintroduced due to the high cooling rates of the substrate.

Selection and peer-review under responsibility of the scientific committee of the 6th CIRP Global Web Conference "Envisaging the future manufacturing, design, technologies and systems in innovation era".

Keywords: Cold Spray; Laser Annealing; Residual Stress; Strain; Strain Gauge Rosette.

1. Introduction

Cold spray (CS) is an additive manufacturing process [1,2] where metallic powders in the range of 1-50 μm are accelerated to velocities of to 1000 m/s in an expanding gas stream. The particles are injected into the supersonic gas stream in a converging-diverging De Laval type nozzle [3,4], as shown in Fig.1. Prior to passing through the nozzle, the gas stream is heated in order to increase the sonic velocity, thus increasing the impact velocity of the particles. As a particle impacts the target surface, it undergoes large plastic deformation and bonds to the surface and/or previous coating layer, allowing thick coatings to be manufactured [5]. The bonding mechanisms in particle-substrate and particle-particle bonding are hypothesised to include phenomena such as mechanical interlocking and adiabatic shear instability [6]. CS is a solid-state process where the melting temperature of the powders are not exceeded, and therefore no material phase change occurs. This ensures the microstructural, mechanical and chemical properties of the particles are retained throughout the process [1,7]. Furthermore, cold spraying can be used on nanocrystalline and amorphous type materials [8,9] and on materials that are sensitive to oxygen inclusion, such as aluminium and copper [8], [10-13].

CS is widely used in the additive manufacturing industry, predominately in coating technologies, such as aerospace,

Selection and peer-review under responsibility of the scientific committee of the 6th CIRP Global Web Conference "Envisaging the future manufacturing, design, technologies and systems in innovation era".
10.1016/j.procir.2018.08.170

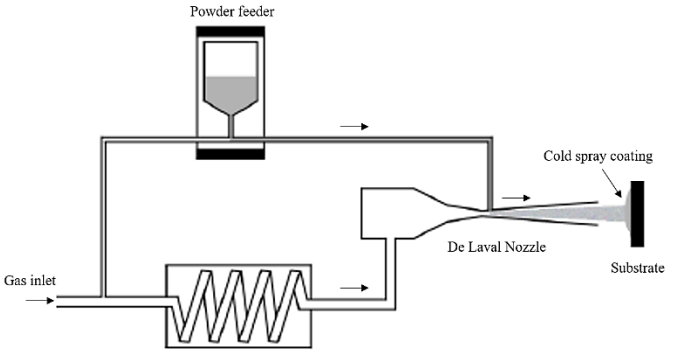

Fig. 1. Cold spray process schematic

medical, automotive and many other fields. CS has been successfully used as a repair process for damaged metal components mainly due to the deposited material's excellent resistance to corrosion, oxidation and high temperatures [14-16] .CS requires a careful selection of parameters in order to achieve adequate coating mechanical properties and the optimal selection of parameters for any task is based of published work and past experiments and results [1], [17,18]. Despite this knowledge on the CS processing parameters and the near 'optimal' choice of parameters, residual stresses can be reduced, however, they will often be present as a result of the plastic deformation experienced during deposition.

Residual stress is defined as the stress that remains within a material when an external force, such as a mechanical/ manufacturing process or thermal gradient, is no longer acting on that material [19]. Residual stresses still remain in a body even when that body is at equilibrium with their surroundings [20]. They are caused through most mechanical and manufacturing processes and in this case, through the CS process, which are predominantly in the form of a compressive residual stress state [21,22]. Compressive residual stresses are generated due to the high velocities and pressures that impact the surface in cold spraying, that causes a large degree of plastic deformation [19]. There have been several studies on the evolution of residual stresses in CS coatings [22–26] and other notable studies will be highlighted. T. Suhonen et al. [27] found that residual stresses were caused by three factors; (i) particle density and deformation behaviour, (ii) difference of the CTEs (coefficient of thermal expansion) of the coating material and substrate, and (iii) temperature, velocity and critical velocity of particles. A. Moridi et al. [28] suggests that the residual stresses are completely compressive due to the low-working temperatures, which also concludes that the number of CS passes has an insignificant effect on the residual stresses in the coating. Whereas, increasing the layer thickness (decreasing the transverse speed, or increase powder feed rate) of the CS coating resulted in the relieving of residual stresses at the interface between the coating and the substrate, however, this increased the compressive residual stresses through the thickness of the coating, thus, decreasing the bond strength. P. Cavaliere et al. [29] found that with the increase of gas pressure and the decrease of temperature, the residual stresses increased. V. Luzin et al. [30] established that compressive residual stress build up is due to the bombardment of particles on the substrate and not from thermal effects, therefore agreeing with A. Moridi et al. [28], that there are no tensile stresses. Ultimately, the residual stresses are from the plastic deformation of the particle during the CS process, hence with higher levels of particle deformation during deposition, leads to higher residual stresses [30].

Residual stress measurement techniques are widely documented, such as; X-ray diffraction (XRD) [31], Neutron diffraction [22], Ultrasonic [32], the Hole Drilling technique [33] and the Contour method [19]. However, these techniques are post-spray measurement techniques, whereas, an in-situ measuring technique would be highly advantageous, similar to the method proposed by B. Marzbanrad, H. Jahed, and E. Toyserkani [26]. Fiber Bragg Grating (FBG) sensors were used to monitor the in-process strains of the CS process, however, it was not linked to residual stress. A method of an in-situ residual stress monitoring tool will be explored in this study. Furthermore, the feasibility of relieving these residual stresses will also be investigated.

Laser annealing is a proposed novel method of relieving residual stresses in CS coatings [34]. The laser offers a high power density over a small area and caters for a large selection of laser parameters. The power level, scanning speed, spot size, laser path and number of passes are some of the parameters of interest in laser heat treatment [35,36]. C. Barile et al. [35] proved the feasibility of stress relief in Aluminium 5068 using laser heat treatment. Furthermore, Pavel A. Podrabinnik and Igor V. Shishkovsky [37] studied the effects of laser annealing on the mechanical properties of the cold spray coating and found that it intensified the intermetallic phase formation and reduced pores and cracks within the coating.

Therefore, in this paper, residual stresses within CS coatings are examined during a laser heat treatment. To achieve this, two novel processes are developed; (i) in-situ residual stress monitoring during CS and laser annealing process, (ii) laser annealing process to relieve residual stresses in CS coatings. This paper aims to build on past publications and to present the feasibility of the two novel processes.

2. Experimental Methodology

2.1. Strain Gauge Rosette

Strain gauge rosettes were used to measure the strain induced during the CS process. CEA-13-120CZ-120 (student class strain gauge rosette), and WK-13-125RA-350 (high temperature strain gauge rosette) were used. The strain gauge rosettes were bonded onto the underside (centre) of a 100 x 100 x 5.57 mm aluminium substrate, where the CS will directly deposit on the opposite side of the substrate over the strain gauge. Adequate substrate preparation was vital prior to the strain gauge bonding. The surface of the substrate was roughened using a crosshatch grinding technique with coarse sandpaper (3M 413Q Paper) and then de-greased (de-greaser/acetone) until clean. The substrate was prepared with M-Prep Conditioner A and M-Prep Neutraliser 5A (Micro-Measurements) to ensure a clean and acid-free surface was obtained and then the strain gauge was glued onto the clean substrate. Further preparation steps were necessary for the high temperature strain gauge rosette; The WK-13-125RA-350 strain gauges were bonded to the aluminium substrates using

M-Bond 600 (Micro-Measurements). A "hot-tack" method of positioning and aligning the strain gauge was used rather than taping, to acquire a more accurate positioning process. The "hot-tack" method utilises a soldering iron to anchor the gauge, and then with Teflon sheets to protect the gauge, it is cured in a furnace (Muffle Furnace, Gallenkamp) for 1 hour 45 minutes at 125 ºC, as specified by Micro-Measurements [38]. Furthermore, high temperature solder (570-28R solder, 93.5% lead, Micro- Measurements) is used to connect lead wires to the data acquisition module (DAQ).

2.2. Strain Reading Module and Data Acquisition

The strain gauge rosettes were connected to a DAQ module (SCXI-1520) and a terminal block (SCXI-1314). The LabView software offered a range of parameters that can be altered to suit the strain gauge type, i.e. CEA-13-120CZ-120 requires 120 Ω, whereas, the WK-13-125RA-350 requires 350 Ω (each gauge therefore needed a hardware change to resistors in Wheatstone bridge). The change in resistance of the gauge due to the induced CS strains is converted to the measured strain values within the LabView software.

2.3. Strain Calculation and Stress Conversion

Eqs. (1)-(2) can be used to determine the principal strains ($\varepsilon_{X,Y}$) in the x and y direction, where the angle to the principal axis (θ) is unknown, given the outputted strains from the DAQ module ($\varepsilon_{1,2,3}$) [38]–[40]. Furthermore, Eqs. (3)-(4) illustrate the conversion from principal strains to principal stresses ($\sigma_{X,Y}$), hence, identifying the percentage change of stress (relieved) during the laser annealing process. Where v is Poisson's ratio and E is the elastic modulus.

$$\boldsymbol{\varepsilon_{X,Y}} = \frac{\boldsymbol{\varepsilon_1 + \varepsilon_2}}{\boldsymbol{2}} \pm \frac{\boldsymbol{1}}{\sqrt{\boldsymbol{2}}}\sqrt{\boldsymbol{(\varepsilon_1 - \varepsilon_2)^2 + (\varepsilon_2 - \varepsilon_3)^2}} \quad (1)$$

$$\boldsymbol{\theta} = \frac{\boldsymbol{1}}{\boldsymbol{2}}\boldsymbol{tan^{-1}}\left(\frac{\boldsymbol{\varepsilon_1 - 2\varepsilon_2 + \varepsilon_3}}{\boldsymbol{\varepsilon_1 - \varepsilon_3}}\right) \quad (2)$$

$$\boldsymbol{\sigma_X} = \frac{\boldsymbol{E}}{\boldsymbol{1 - \nu^2}}\boldsymbol{(\varepsilon_X + \nu\varepsilon_Y)} \quad (3)$$

$$\boldsymbol{\sigma_Y} = \frac{\boldsymbol{E}}{\boldsymbol{1 - \nu^2}}\boldsymbol{(\varepsilon_Y + \nu\varepsilon_X)} \quad (4)$$

2.4. Standardised Rig

A standardised rig (Fig. 2) was developed to allow for consistent and repeatable tests. The clamping system incorporated a pinned support system rather than a fixed clamp, which permitted bending of the substrate, whereas a fixed support prohibits bending and can lead to an increased apparent stiffness of the substrate reducing the strain levels measured. Therefore, under the pressure of the CS process, the substrate can bend and then retain its original shape after the CS process. This ensures that there is minimal plastic deformation of the substrate, since any deformation will change the stress state.

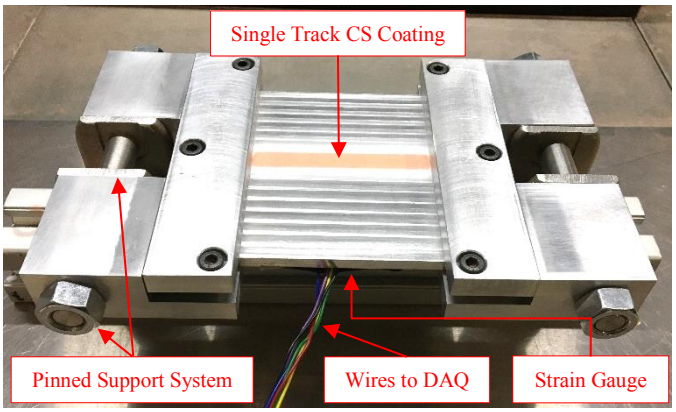

Fig. 2. CS process clamping system (including wires connected to strain gauge rosette and DAQ module).

Table 1. CS processing parameters.

Powder	Pressure [bar]	Temperature [ºC]	Transverse Speed [mm/s]	PFR* [%]	SoD** [mm]
Cu	30	600	50	30	40

Note: *PFR = Particle Feed Rate; **SoD = Standoff Distance.

Table 2. Laser annealing processing parameters

Test	Speed [mm/s]	Number of Passes	Power [w]	Strain Gauge Selection*	Substrate Clamped
1	3	2	105	A	Yes
2	3	4	105	A	Yes
3	3	8	105	A	Yes
4	3	2	105	A	No
5	6	2	66	A	No
6	6	4	66	A	No
7	6	8	66	A	No
8	3	4	66	A	No
9	6	2	105	A	No
10	6	4	105	A	No
11	6	8	105	A	No
12	3	2	105	B	No
13	3	4	105	B	No
14	3	8	105	B	No
15	Furnace Stress Relieving. 180ºC for 1hr [41]			B	No

Note: *Strain gauge: A = CEA-13-120CZ-120, B = WK-13-125RA-350

2.5. CS and Laser Annealing Processing Parameters

The testing consisted of 15 100 x 100 x 5.57 mm square aluminium substrates which were cold sprayed with spherical copper (Cu) powders (-38+15 mm, Safina, Czech Republic). Each substrate had guidelines which aids strain gauge rosette placement and to improve experimentation repeatability. The CS process was conducted in Trinity College using an in-house CS system, where a single track of Cu was sprayed. The CS parameters are shown in Table 1, where the gas type was

helium (He). These parameters were chosen to achieve a coating thickness of ~400 µm. The developed clamping system was fixed in the CS machine and the processing parameters were also fixed, ensuring consistent testing. Post spraying, the samples were spray painted matte black in preparation for the laser process.

The laser annealing process was conducted on a 150 W BRM 90130 CO_2 laser where the processing parameters are based on prior experiments [34], as seen Table 2. The laser spot diameter was ~6 mm and followed a zigzag pattern.

3. Results and Discussion

3.1. CS In-Situ Strain Monitoring

The novel strain gauge rosette method of measuring the in-situ strains induced by the CS process proved to be a consistent and reliable approach that can be used as monitoring tool for predicting the magnitude of residual stress build up during CS. Fig. 4 (a) presents the in-situ strains of the CS process. The CS induces a negative strain which represents the compressive residual stresses. The strains reach steady state and there is residual strain within the substrate after manufacture, indicating the residual stress left within the CS coating. After numerous tests, the strains at steady state are consistent and prove that this novel approach is repeatable. Thus allowing for the comparison of different parameters to optimise the CS process by minimising and monitoring residual stress build up.

3.2. Laser Annealing

Table 2 shows the laser annealing parameters which were varied, and the levels used. The preliminary in-clamp laser annealing tests (Tests: 1-3) proved that since annealing is a temperature dependant process, the subject sample requires expansion and contraction to undergo a stress relieving heat treatment cycle. Tests 1-3 show that no stress relieving can occur when the substrate and coating are restricted to expand and/or contract. The in-situ strains of the full test can be seen in Fig. 3. The remaining tests focused on the change of power and laser/power exposure time.

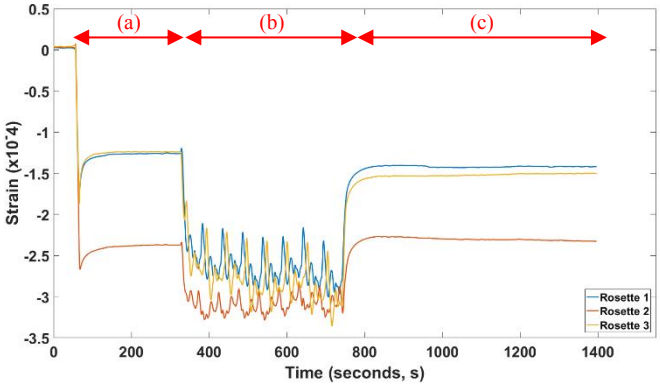

Fig. 3. Test 3 in-situ strains. (a) CS process, (b) laser annealing process, (c) steady state.

Tests 5-7 showed that with low power, higher number of passes are required to have any effect on the coating, as expected. There was virtually no difference in strain at steady state after 2 and 4 passes respectively (similar to Fig. 3). This Indicates that the coating was not exposed to the laser power for a sufficient enough time for any annealing effects to occur. However, after 8 passes at low power produced a negative effect on the coatings strain rates, due to the lack of temperature compensation in CEA-13-120CZ-120 type strain gauge.

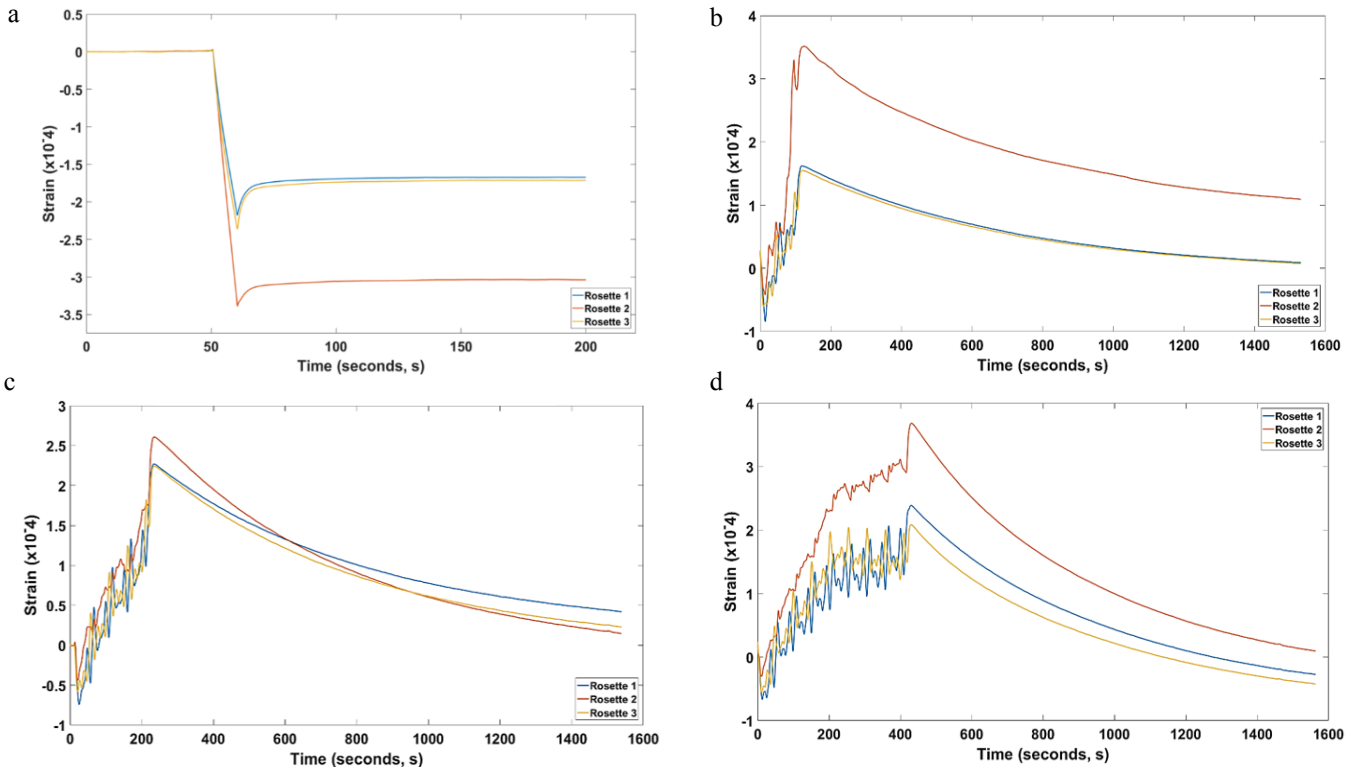

Fig. 4. Measured in-situ strains: (a) CS strains, (b) laser annealing strains - Test 12, (c) laser annealing strains - Test 13, (d) laser annealing strains - Test 14.

Tests 9-11 were conducted at a higher power, where the power density experienced by the coating is nearly doubled in these tests. At this speed, power and number of passes, test 9 again proved that there is not sufficient enough power exposed to the coating. Therefore, no annealing can occur. Furthermore, similar to test 7, tests 10-11 do not offer any conclusive results due to negative effects of the laser annealing process. The reasons why the laser annealing process is not working in this case is due to exceeding the strain gauge's maximum temperature, insufficient laser exposure and possibly the scanning strategy only annealing surface above the strain gauge. Therefore, tests 12-15 will use the high precision, high temperature strain gauge rosettes.

3.3. Laser Annealing – High Temperature Strain Gauge

Tests 12-14 analysed slower speeds so the coating can experience larger power densities and exposure times. Under these conditions, a relieving of strain was obtained during the process. Fig. 4 (b-d), provide results from the high temperature strain gauge laser annealing. On all graphs, the laser has a positive effect on the strain during the process, indicating that the laser is heat treating the coating, and thus, relieving the residual stresses. The results show a linear relationship between the laser energy applied to the surface and the level of stress relief shown in the strain results. This now illustrates that even after only 2 passes of the laser, the scale of the graph matches that of the negative cold spray strains, as seen in Fig. 4 (a), and therefore, at the end of the laser heat treatment, the strains have been completely relieved. This proves the viability and possibility of the use of laser annealing to relieve residual stresses in CS coatings. The negative strains induced through the CS process (Fig. 4 (a)) are completely relieved during the laser annealing process by the positive strains during that process (Fig. 4 (b-d)).

However, in reality, the strain relieving appears to be cancelled out as the strain levels fall back to the original negative state after the laser process. Using higher temperature compensated strain gauges could show the real reduction of residual stresses. The strains are reintroduced due to the high cooling rates of the substrate, that introduces tensile residual stresses into the coating [28]. Although, at steady state after the laser annealing process, there is not a reduction in residual strains in the coating, the feasibility of this novel method of stress relieving is confirmed through a standard stress relieving furnace cycle according to ASM International [41]. The Cu coating was subjected to 180ºC for 1 hour to relieve the residual stress. Fig. 5 illustrates the results. Section (a) on Fig. 5, mimics the stress relieving sections on Fig. 4 (b-d), showing the relieving of strains within the coating during the stress relieving cycle. Therefore, proving the possibility of laser annealing as a tool to relieve residual stresses, since this method is directly comparable to the control test (ASM International stress relieving furnace cycle for copper [41]).

Due to the similarities of the final curve to steady state between the standard stress relieving furnace cycle (Fig. 5), and the three laser stress relieving experiments (high temperature strain gauges, 12-14, Fig. 4 (b-d)), it suggests that the reason for the reintroduction of strains into the coating are related to

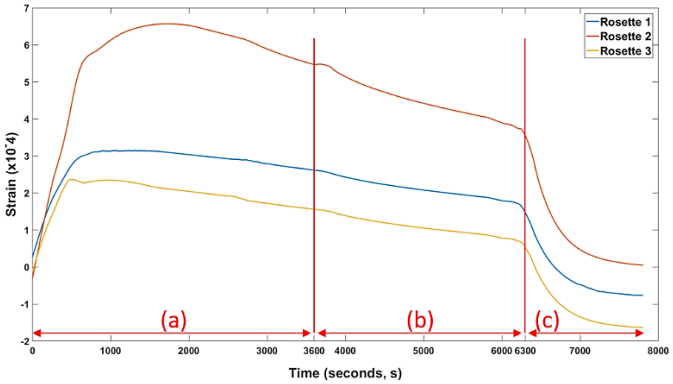

Fig. 5 Furnace stress relieving at 180ºC for 1 hour, in-situ stains: (a) 180ºC for 1 hour, (b) 45-minute cooling in furnace, (c) room air temperature cooling until steady state.

the high cooling rates of the substrate (depicted (c) on Fig. 5). This again shows the viability of laser annealing on the residual stresses in CS coatings. However, for this particular geometry and experimental setup, the relieved strains are reintroduced due to contraction effects of the cooling substrate. Further investigation is required to compare the cooling rate effects against the reintroduced strains, where slower cooling rates can result in lower average maximum residual stress magnitudes [28,42]. Therefore, either larger substrates or CS coatings could lead to slower cooling rates and thus, less reintroduced strains.

3.4. Future Work

Future work will focus on the optimisation of the CS process using strain gauges to minimise residual stresses in CS deposits. Experimentation of numerous CS scanning strategies, speeds, materials, passes and temperatures will determine the effects of each parameter on the in-situ residual stresses. Therefore, minimising the residual stresses and negating the need for post-processing. Additionally, the optimisation of the laser annealing process using the high temperature strain gauges to analyse the effects of different cooling rates on the reintroduced strains will be examined.

4. Conclusion

The effects of laser annealing on a single track of copper CS deposition was investigated. This paper focuses on studying the effects of laser annealing on the residual stresses and thus, determining the feasibility of using a laser for stress relieving purposes. In-situ strain evolution was monitored during the CS and laser annealing processes, using a novel rectangular strain gauge rosette technique. This paper found:

1. The measured in-situ CS strains were accurate and consistent, proving to be a viable monitoring tool for residual stress development during the CS process.
2. Laser annealing proved to be a viable process in the relieving of residual stresses in CS coatings. In-situ testing using high-temperature strain gauges found that the residual stresses are completely relieved during laser annealing.

3. The high cooling rates after the laser and furnace annealing processes reintroduced strains back into the coating, appearing to cancel out the stress relieving achieved by the laser. However, it is believed that if the cooling rates are controlled and more strain gauge temperature compensations are considered, it is possible to negate the negative effects experienced during the cooling phases.

References

[1] R. N. Raoelison et al., "Cold gas dynamic spray technology: A comprehensive review of processing conditions for various technological developments till to date," Addit. Manuf., vol. 19, pp. 134–159, 2018.

[2] A. Sova, S. Grigoriev, A. Okunkova, and I. Smurov, "Potential of cold gas dynamic spray as additive manufacturing technology," Int. J. Adv. Manuf. Technol., vol. 69, no. 9–12, pp. 2269–2278, 2013.

[3] E. Irissou, J.-G. Legoux, A. N. Ryabinin, B. Jodoin, and C. Moreau, "Review on Cold Spray Process and Technology: Part I—Intellectual Property," J. Therm. Spray Technol., vol. 17, no. 4, pp. 495–516, 2008.

[4] S. Grigoriev, A. Okunkova, A. Sova, P. Bertrand, and I. Smurov, "Cold spraying: From process fundamentals towards advanced applications," Surf. Coatings Technol., vol. 268, pp. 77–84, 2015.

[5] R. C. Dykhuizen and M. F. Smith, "Gas Dynamic Principles of Cold Spray," J. Therm. Spray Technol., vol. 7, no. 2, pp. 205–212, 1998.

[6] H. Assadi, F. Gärtner, T. Stoltenhoff, and H. Kreye, "Bonding mechanism in cold gas spraying," Acta Mater., vol. 51, no. 15, pp. 4379–4394, 2003.

[7] T. Schmidt et al., "From particle acceleration to impact and bonding in cold spraying," J. Therm. Spray Technol., vol. 18, no. 5–6, pp. 794–808, Dec. 2009.

[8] Q. Wang, N. Birbilis, and M. X. Zhang, "Interfacial structure between particles in an aluminum deposit produced by cold spray," Mater. Lett., vol. 65, no. 11, pp. 1576–1578, Jun. 2011.

[9] L. Ajdelsztajn, J. M. Schoenung, B. Jodoin, and G. E. Kim, "Cold spray deposition of nanocrystalline aluminum alloys," Metall. Mater. Trans. A, vol. 36, no. 3, pp. 657–666, Mar. 2005.

[10] K. Balani, T. Laha, A. Agarwal, J. Karthikeyan, and N. Munroe, "Effect of carrier gases on microstructural and electrochemical behavior of cold-sprayed 1100 aluminum coating," Surf. Coatings Technol., vol. 195, no. 2–3, pp. 272–279, May 2005.

[11] Z. Arabgol, M. Villa Vidaller, H. Assadi, F. Gärtner, and T. Klassen, "Influence of thermal properties and temperature of substrate on the quality of cold-sprayed deposits," Acta Mater., vol. 127, pp. 287–301, 2017.

[12] A. Sova, S. Grigoriev, A. Okunkova, and I. Smurov, "Cold spray deposition of 316L stainless steel coatings on aluminium surface with following laser post-treatment," Surf. Coatings Technol., vol. 235, pp. 283–289, 2013.

[13] M. R. Rokni, C. A. Widener, and V. R. Champagne, "Microstructural stability of ultrafine grained cold sprayed 6061 aluminum alloy," Appl. Surf. Sci., vol. 290, pp. 482–489, 2014.

[14] S. Yin, P. Cavaliere, B. Aldwell, R. Jenkins, H. Liao, and W. Li, "Cold spray additive manufacturing and repair: Fundamentals and applications," Addit. Manuf., vol. 21, no. April, pp. 628–650, 2018.

[15] V. K. Champagne and D. J. Helfritch, "Mainstreaming cold spray – push for applications," Surf. Eng., vol. 30, no. 6, pp. 396–403, Jun. 2014.

[16] A. M. Vilardell, N. Cinca, A. Concustell, S. Dosta, I. G. Cano, and J. M. Guilemany, "Cold spray as an emerging technology for biocompatible and antibacterial coatings: state of art," J. Mater. Sci., vol. 50, no. 13, pp. 4441–4462, Jul. 2015.

[17] W. Y. Li and C. J. Li, "Optimal design of a novel cold spray gun nozzle at a limited space," Journal of Thermal Spray Technology, vol. 14, no. 3. pp. 391–396, 2005.

[18] W.-Y. Li and C.-J. Li, "Optimization of spray conditions in cold spraying based on numerical analysis of particle velocity," Trans. Nonferrous Met. Soc. China (English Ed., vol. 14, no. 2, pp. 43–48, Oct. 2004.

[19] N. S. Rossini, M. Dassisti, K. Y. Benyounis, and A. G. Olabi, "Methods of measuring residual stresses in components," Mater. Des., vol. 35, pp. 572–588, 2012.

[20] X. Huang, Z. Liu, and H. Xie, "Recent progress in residual stress measurement techniques," Acta Mech. Solida Sin., vol. 26, no. 6, pp. 570–583, 2013.

[21] A. Moridi, S. M. Hassani-Gangaraj, M. Guagliano, and S. Vezzu, "Effect of cold spray deposition of similar material on fatigue behavior of Al 6082 alloy," in Conference Proceedings of the Society for Experimental Mechanics Series, 2014, vol. 7, pp. 51–57.

[22] K. Spencer, V. Luzin, N. Matthews, and M. X. Zhang, "Residual stresses in cold spray Al coatings: The effect of alloying and of process parameters," Surf. Coatings Technol., vol. 206, no. 19–20, pp. 4249–4255, 2012.

[23] V. Luzin, K. Spencer, and M. X. Zhang, "Residual stress and thermo-mechanical properties of cold spray metal coatings," Acta Mater., vol. 59, no. 3, pp. 1259–1270, 2011.

[24] S. Sampath, X. Y. Jiang, J. Matejicek, L. Prchlik, A. Kulkarni, and A. Vaidya, "Role of thermal spray processing method on the microstructure, residual stress and properties of coatings: An integrated study of Ni-5 wt. % Al bond coats," Mater. Sci. Eng. A, vol. 364, no. 1–2, pp. 216–231, Jan. 2004.

[25] W. B. Choi et al., "Integrated characterization of cold sprayed aluminum coatings," Acta Mater., vol. 55, no. 3, pp. 857–866, Feb. 2007.

[26] B. Marzbanrad, H. Jahed, and E. Toyserkani, "On the evolution of substrate's residual stress during cold spray process: A parametric study," vol. 138, pp. 90–102, 2018.

[27] T. Suhonen, T. Varis, S. Dosta, M. Torrell, and J. M. Guilemany, "Residual stress development in cold sprayed Al, Cu and Ti coatings," Acta Mater., vol. 61, no. 17, pp. 6329–6337, 2013.

[28] A. Moridi, S. M. Hassani Gangaraj, S. Vezzu, and M. Guagliano, "Number of passes and thickness effect on mechanical characteristics of cold spray coating," Procedia Eng., vol. 74, pp. 449–459, 2014.

[29] P. Cavaliere and A. Silvello, "Processing conditions affecting residual stresses and fatigue properties of cold spray deposits," Int. J. Adv. Manuf. Technol., vol. 81, no. 9–12, pp. 1857–1862, Dec. 2015.

[30] V. Luzin, K. Spencer, and M.-X. Zhang, "Residual stress and thermo-mechanical properties of cold spray metal coatings," Acta Mater., vol. 59, no. 3, pp. 1259–1270, Feb. 2011.

[31] M. Kato, M. Nazul, T. Itti, H. Akebono, A. Sugeta, and E. Mitani, "Effects of coating thickness and interfacial roughness on cracking and delamination strength of WC-Co coating measured by ring compression test," in IOP Conference Series: Materials Science and Engineering, 2014, vol. 61.

[32] Q. Wang, X. Liu, Z. Yan, Z. Dong, and D. Yan, "On the mechanism of residual stresses relaxation in welded joints under cyclic loading," Int. J. Fatigue, vol. 105, pp. 43–59, 2017.

[33] K. Mathar, "Determination of Initial Stresses by Measuring the Deformations Around Drilled Holes," Trans. Am. Soc. Mech. Eng., pp. 249–254, 1934.

[34] B. Aldwell, B. Hunter, R. Jenkins, and R. Lupoi, "Fundamental Investigation into the Effects of In-process Heat Treatment in Cold Spray," in International Thermal Spray Conference 2018, 2018, pp. 227–232.

[35] C. Barile, C. Casavola, G. Pappalettera, and C. Pappalettere, "Feasibility of Local Stress Relaxation by Laser Annealing and X-ray Measurement," Strain, vol. 49, no. 5, pp. 393–398, 2013.

[36] I. A. Palani, N. J. Vasa, M. Singaperumal, and T. Okada, "Investigation on laser-annealing and subsequent laser-nanotexturing of amorphous silicon (a-Si) films for photovoltaic application," J. Laser Micro Nanoeng., vol. 5, no. 2, pp. 150–155, 2010.

[37] P. A. Podrabinnik and I. V. Shishkovsky, "Laser Post Annealing of Cold-Sprayed Al–Ni Composite Coatings for Green Energy Tasks," Mater. Sci. Forum, vol. 834, pp. 113–118, 2015.

[38] N. Instruments, "SCXI-1520 User Manual," no. 372583E–01, 2009.

[39] J. M. Gere, Mechanics of Materials, 6th Editio. Bill Stenquist, 2008.

[40] Micro-Measurements, "Strain Gage Rosettes: Selection, Application and Data Reduction," no. c, pp. 1–12, 2014.

[41] H. Chandler et al., "Heat Treater's Guide. Practices and Procedures for Nonferrous Alloys," ASM Int., p. 669, 1996.